

Bottomonia suppression in heavy-ion collisions from AdS/CFT

N N Barnard and W A Horowitz

Department of Physics, University of Cape Town, Private Bag X3, Rondebosch 7701, South Africa

E-mail: brnnad007@myuct.ac.za

Abstract. We compute for the first time the suppression of bottomonia in a strongly coupled QGP and compare the results to those from a weakly coupled QGP and to data. Using imaginary time techniques we numerically determine the real and imaginary parts of the binding energy of ground state bottomonia in a potential computed from AdS/CFT and another computed from pQCD. We implement the complex binding energies in a suppression model to determine the $\Upsilon(1S)$ nuclear modification factor in $\sqrt{s_{NN}} = 2.76$ TeV Pb+Pb collisions. This simplest strong-coupling, p_T -independent potential leads to a significant oversuppression of $\Upsilon(1S)$ compared to data while the results from the pQCD-derived potential are consistent with data. We also investigate the validity of using complex heavy quark potentials from AdS/CFT for all quark separation r by independently computing the meson spectrum using semiclassical, rotating open strings attached to the D7-brane.

1. Introduction

The relativistic heavy-ion collisions at the Large Hadron Collider (LHC) and the Relativistic Heavy Ion Collider (RHIC) are sufficiently energetic for hadrons to transition into a new phase of colored matter, known as the quark-gluon plasma (QGP) [1]. In vacuum, quarkonia are bound states of a heavy quark and its anti-quark pair [2]. Embedded in a medium, the properties of quarkonia change. Matsui and Satz [3] were the first to propose that quarkonia may theoretically exist in conjunction with the QGP at $T > T_c$, where T_c is the critical temperature required for QGP formation, due to its small binding radii relative to the screening radius, whereas lighter hadrons dissociate at $\sim T_c$. At some T , the screening radius becomes smaller than the typical quarkonia radii, leading to their dissolution. In addition, excited states of quarkonia dissociate before the ground state [4]. The suppression of the bound states of quarkonia in heavy-ion collisions is hence a valuable indicator of the formation of QGP, and the comparison of the quarkonia spectra in high multiplicity collisions to that in minimum bias $p + p$ collisions where no QGP is formed is a useful probe of the QGP's properties.

Potential models can be used to describe the interaction of the quark and antiquark in the $q\bar{q}$ pair to calculate the suppression of quarkonia production in heavy-ion collisions [3]. This potential at finite temperature contains not only a standard real Debye-screened term, but also an imaginary part which gives the thermal width of the state, and hence its suppression [5]. One of the first to show this was [6], which made use of perturbative methods to find the static potential of quarkonia at finite temperature. They concluded that the thermal width of the

state increases with T , suggesting that at high T the dissociation due to the effect described by the imaginary part of the potential occurs before color screening can even come into effect.

The complex-valued potential was explored further using non-perturbative lattice QCD by [5], among others, allowing for the study of strongly-coupled quarkonia as well. An important consideration in finding heavy quarkonium suppression is the velocity of the $q\bar{q}$ in relation to the surrounding QGP, however, while perturbative and lattice QCD calculations generally consider the $q\bar{q}$ meson to be at rest in the medium.

The suppression of quarkonia moving at velocity in a QGP hence requires holographic techniques such as the Anti-de Sitter/Conformal Field Theory (AdS/CFT) correspondence. Liu, Rajagopal and Wiedemann (LRW) [7] were the first to present a quantitative description from AdS/CFT of the consequences of velocity on the screening length of charmonium, suggesting that for strongly coupled J/ψ , velocity could result in a significant additional source of suppression at high transverse momentum p_T in the form of a decrease in dissociation energy with increased velocity. Since then, many have performed similar investigations, and while the aforementioned are limited in their scope of application, it is interesting to note that [8] in particular concludes that the effect of velocity may not be as consequential as postulated in LRW.

We would ultimately like to investigate the consequences of these different velocity dependence pictures from AdS/CFT compared to pQCD. Here we have a more modest goal: to compare the experimentally measurable consequences of pQCD vs. AdS/CFT pictures.

2. Potential Models

The potential model for weakly coupled quarkonia is taken from [9]. We plot the real and imaginary parts of the weakly coupled potential as a function of quark separation r for various temperatures in figures 1a and 1b, respectively.

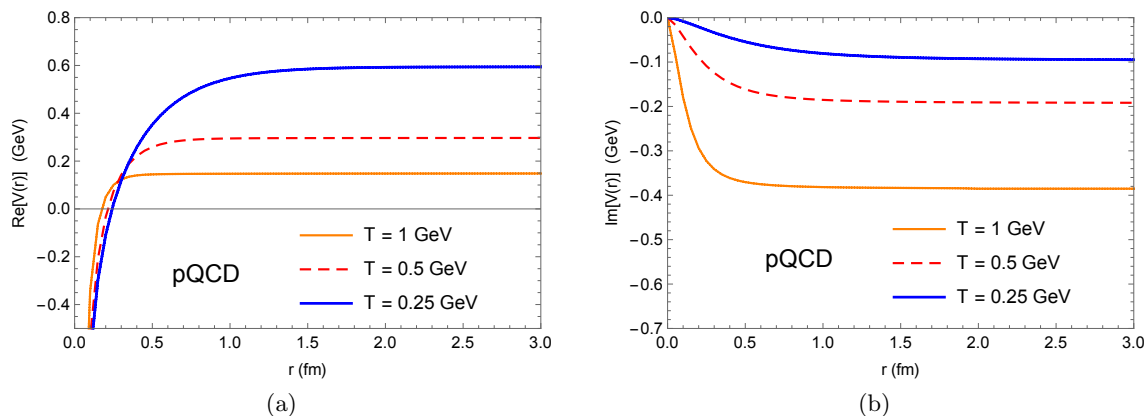


Figure 1. Plot of the (a) real part and the (b) imaginary part of the weakly coupled potential, as a function of the distance r between the quark and anti-quark in the $b\bar{b}$, for various T .

We modeled the strongly coupled quarkonia at rest in a QGP with the potential given in Albacete et al. [10], which was derived in $\mathcal{N} = 4$ super Yang-Mills at finite temperature using AdS/CFT. Note that the potential becomes complex for $r > r_c \simeq 0.870/\pi T$. Considering that both weakly coupled pQCD and non-perturbative lattice QCD methods yield complex heavy quark potentials, it is sensible to expect the same using AdS/CFT methods. We provide further supporting evidence for our procedure in Section 4, which gives an independent calculation of the binding energies for $\Upsilon(1S)$ using semiclassical, rotating open strings attached to the D7-brane.

Figure 2a and 2b show the real and imaginary parts of the strongly coupled potential as a function of quark separation r taking $\lambda = 10$.

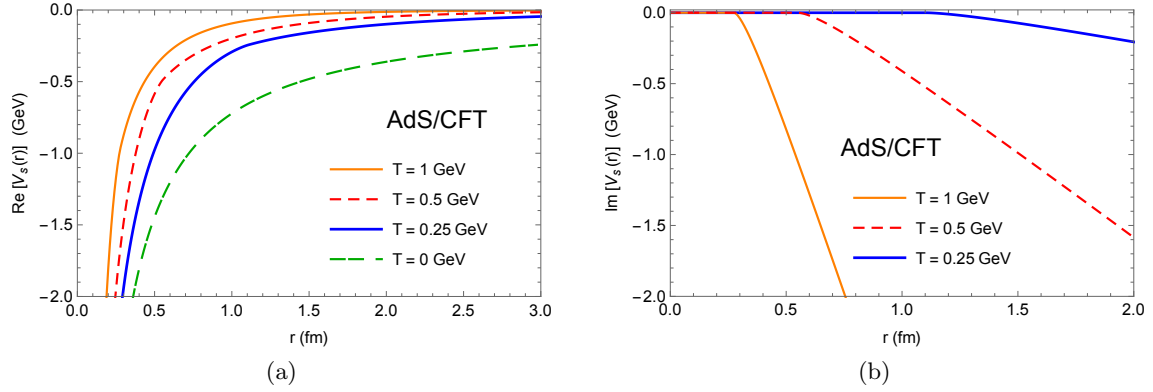


Figure 2. The (a) real part and the (b) imaginary part of the strongly coupled potential, as a function of the distance r between the quark and anti-quark in the $b\bar{b}$, for various temperatures T .

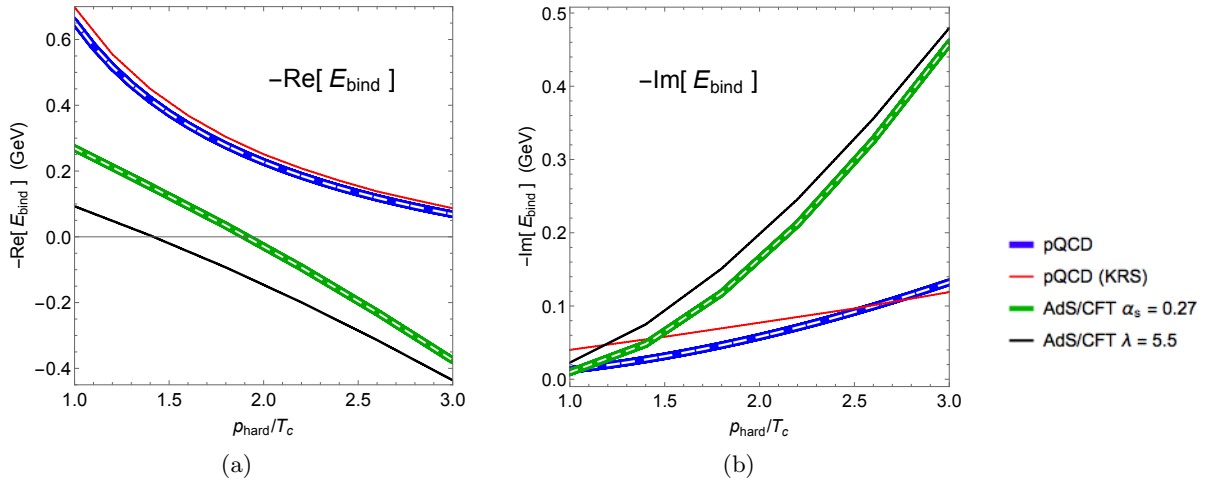


Figure 3. The (a) negative real part and (b) negative imaginary part of E_{bind} for $\Upsilon(1S)$. The dashed white curves inside the blue and green curves are from the independent evaluation using the complex variational method.

3. Binding Energies

The imaginary time numerical method used to calculate the binding energies from the potential models given in Section 2 follows that of [9, 11], with modifications (see [12] for details). Figure 3a gives the real part of the binding energy of $\Upsilon(1S)$ from the pQCD potential and AdS/CFT potential, as a function of temperature. Figure 3b gives the imaginary part of E_{bind} .

For the AdS/CFT results, we show the binding energy both for the case where the coupling constant is $\lambda = 10$ (labeled as $\alpha_s = 0.27$) and where $\lambda = 5.5$; the reasoning behind the choice of these values is explained in [12]. The binding energy results for bottomonium from [11] are labeled “pQCD (KRS)” and are included for comparison.

Both the binding energy results presented for the pQCD potential and the AdS/CFT potential taking $\lambda = 10$ were independently confirmed using a complex variational method; see Appendix A of [12] for details.

The binding energy found from our adapted methodology for the pQCD potential differs quantitatively from that presented in [11], which was used in Kroupa et al. [9] to calculate suppression. In the case of $\Upsilon(1S)$, this difference does not change the qualitative behavior of the quarkonia, since both results suggest that the quarkonia remain bound up to at least $T = 3T_c$.

However, we will see in Section 5 that the small quantitative differences in the derived binding energies lead to a significant quantitative difference in the predicted suppression.

4. Comparison to an Independent Alternative Method: Hanging, Rotating Strings

We seek an independent confirmation of the binding energies given in Section 3 computed using the non-relativistic imaginary time numerical method [12], using the potential from AdS/CFT as given in figure 2.

Kruczenski et al. [13] computes the energy spectrum of mesons at $T = 0$ from semiclassical, rotating open strings attached to a D7-brane. In particular, in the limit $J \gg \sqrt{\lambda}$, where J is the spin, [13] notes that the spectrum corresponds to that of a non-relativistic $q\bar{q}$ -pair bound by a Coulomb potential. We extended the results from [13] to $T > 0$. In addition, we generalized the complex strongly coupled potential from Albacete et al. [10], which was derived in the infinite mass limit, to finite mass. We then compared the binding energies found using this generalized finite mass potential with the non-relativistic numerical regime (NRQM) with the binding energies from the semiclassical string method (SSM).

For the simplest $T = 0$ case, both the binding energies from the SSM and NRQM are purely real. These binding energies are shown in figure 4a for a range of quark masses. The binding energies from the two methods agree for large J . At small J , however, $E_{\text{bind}}^{\text{NRQM}} > E_{\text{bind}}^{\text{SSM}}$.

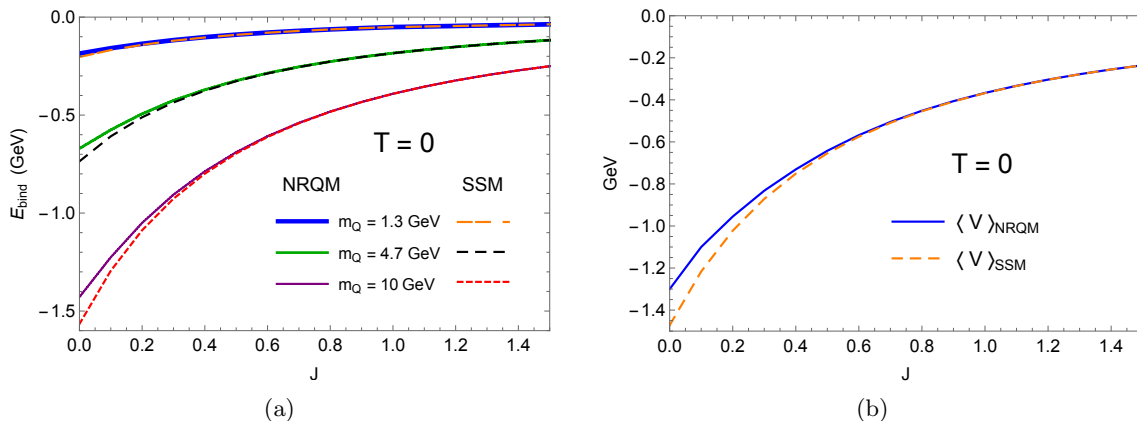


Figure 4. (a) The binding energies from NRQM and SSM for a range of quark masses m_Q . (b) The average potential $\langle V \rangle_{\text{NRQM}}$ from NRQM and $\langle V \rangle_{\text{SSM}}$ from the SSM for $m_Q = 4.7$ GeV.

This discrepancy occurs since the imaginary time numerical method takes into account quantum spreading of the wavefunction, whereas the SSM does not. We may explicitly demonstrate the effect of this quantum spreading by investigating the potential probed by the two methods. We show in figure 4b the average potential felt by the heavy quarks in the two methods. It is evident from figure 4b that $\langle V \rangle_{\text{NRQM}} > \langle V \rangle_{\text{SSM}}$: the average potential experienced by the heavy quarks is deeper at small J for the SSM as opposed to NRQM. We may understand the ordering of potentials from the quantum spreading – the NRQM wavefunction preferentially explores the potential at larger r due to uncertainty. As a result, the binding energies are therefore less negative when quantum effects are taken into account, i.e. the quarkonia is less strongly bound, as expected.

Figure 5a and 5b show the real and imaginary parts, respectively, of the binding energies from NRQM and the SSM for $\Upsilon(1S)$ for a range of temperatures. At small J , the real part of the NRQM binding energy is slightly larger than the real part of the binding energy from the SSM, as was the case for $T = 0$.

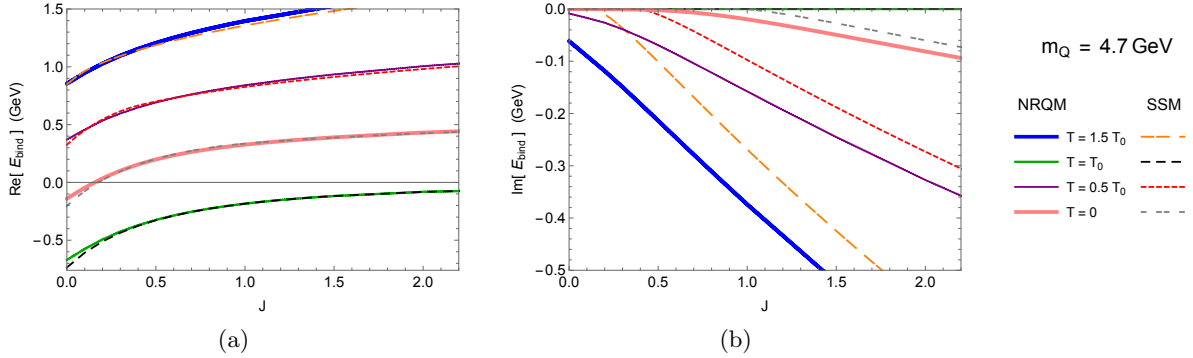


Figure 5. The (a) real and (b) imaginary parts of E_{bind} of $\Upsilon(1S)$ for a range of T .

The imaginary part of the E_{bind} echo the conclusions drawn regarding the difference in the real parts. The binding energies from NRQM become complex at smaller J than those from the SSM. The larger the imaginary part of the binding energy, the greater the tendency for the quarkonia to fall apart: the $\Upsilon(1S)$ in the NRQM picture is again less tightly bound than SSM.

For large J , however, the binding energies converge as expected. The excellent agreement of these binding energies shows that the use of complex heavy quark potentials to compute binding energies is consistent with the independent semiclassical string method.

5. Suppression

We would lastly like to make quantitative predictions for the suppression of bottomonia in heavy ion collisions and compare to measured data. The nuclear modification factor R_{AA} is calculated following [9] – see [12] for details.

Figure 6a gives the nuclear modification factor R_{AA} for each of the sets of binding energies shown in figure 3a and 3b as a function of the number of participating nucleons N_{part} . Figure 6b shows $R_{AA}(p_T)$, where all centrality classes are included, weighed by the number of binary nucleon-nucleon collisions N_{coll} . Suppression results for mid-rapidity ($|y| < 2.4$) Pb+Pb collisions at $\sqrt{s_{NN}} = 2.76$ TeV from the CMS Collaboration [14] are included in figure 6a and 6b for comparison.

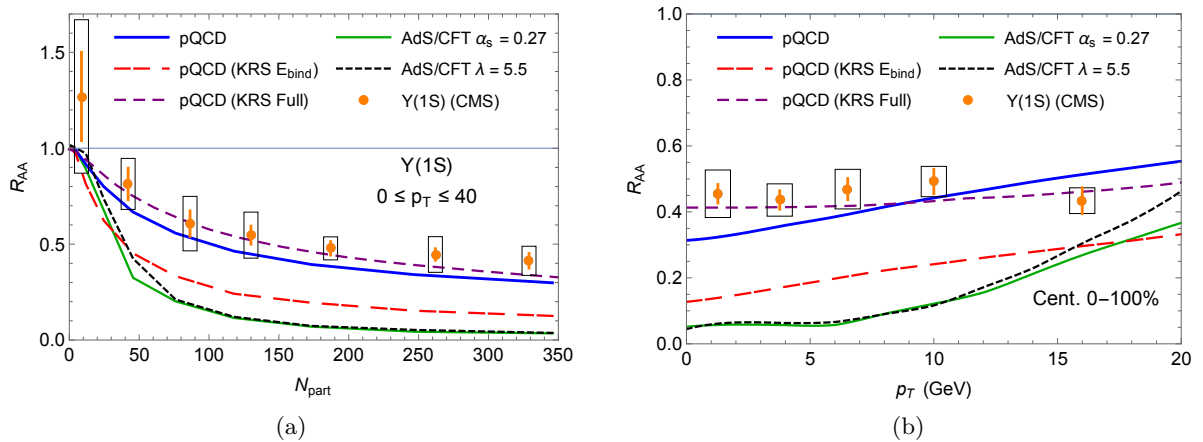


Figure 6. (a) Nuclear modification factor R_{AA} as a function of the number of participating nucleons N_{part} for $0 \leq p_T \leq 40$. (b) Nuclear modification factor R_{AA} as a function of transverse momentum p_T for combined centrality classes. Data from CMS [14] is included in orange.

6. Discussion and Outlook

We present the suppression of $\Upsilon(1S)$ computed for the first time in an isotropic strongly coupled QGP, compare the results to those from a weakly coupled QGP, and to data [14].

Our first results for $\Upsilon(1S)$ strongly coupled to a strongly coupled plasma show binding energies with much larger imaginary parts than those found from the pQCD potential, as well as real parts that become positive within the T_c to $3T_c$ range considered. Thus, for the potential models considered here, a strongly coupled $\Upsilon(1S)$ interacting with a strongly coupled plasma melts at a *lower temperature* than a weakly coupled $\Upsilon(1S)$ interacting with a weakly coupled plasma. The $\Upsilon(1S)$ hence appears more strongly bound at weak coupling than at strong coupling, which is surprising.

Quantitatively, our full model—comprised of the potential, the resulting quarkonia E_{bind} , and the translation to R_{AA} —significantly overpredicts the suppression of strongly coupled $\Upsilon(1S)$ compared to data. Our predictions for weakly coupled $\Upsilon(1S)$ are consistent with data.

We note that our model for the medium is significantly less sophisticated compared to that used in [9]: our background is an optical Glauber model as opposed to the 3+1D viscous anisotropic hydrodynamics in that work. Our medium incorporates only Bjorken expansion, whereas the background in [9] includes transverse expansion and entropy production. Therefore the plasma in [9] cools faster than ours, leading to our model showing more dissociation for the same binding energies. The extent of the sensitivity of R_{AA} to the background used is surprisingly large. With the only difference being the background geometry used, we ran the binding energies from [11] through our suppression model and found an R_{AA} a factor of two smaller than that shown in [9].

In contrast to the favorable comparison between the pQCD-based results of [9] and the CMS data [14], if we assume our weak coupling binding energies are more accurate than those of [11], then computing R_{AA} with the more sophisticated background from [9] would likely yield a significant underprediction of the suppression of bottomonia.

At strong coupling, with a potential derived from AdS/CFT as described in [10], it seems unlikely that the use of a more sophisticated background would reduce the suppression of bottomonia enough that the predicted R_{AA} would be consistent with data; however, the differences from using a more sophisticated background, suppression model, and velocity dependent potential may ultimately be sufficient for future strongly coupled quarkonia predictions to be consistent with current data.

Acknowledgments

The authors thank the South African National Research Foundation and SA-CERN Consortium for their financial support. The authors also thank Michael Strickland for useful discussions.

References

- [1] Gyulassy M and McLerran L 2005 *Nucl. Phys. A* **750** 30–63
- [2] Patrignani C et al. (Particle Data Group) 2016 *Chin. Phys. C* **40** 100001
- [3] Matsui T and Satz H 1986 *Phys. Lett. B* **178** 416–22
- [4] Karsch F, Kharzeev D and Satz H 2006 *Phys. Lett. B* **637** 75–80
- [5] Rothkopf A, Hatsuda T and Sasaki S 2012 *Phys. Rev. Lett.* **108** 162001
- [6] Laine M, Philipsen O, Romatschke P and Tassler M 2007 *J. High Energy Phys.* JHEP03(2007)054
- [7] Liu H, Rajagopal K and Weidemann U A 2007 *Phys. Rev. Lett.* **98** 182301
- [8] Finazzo S I and Noronha J 2015 *J. High Energy Phys.* JHEP01(2015)051
- [9] Krouppa B, Ryblewski R and Strickland M 2015 *Phys. Rev. C* **92** 061901
- [10] Albacete J L, Kovchegov Y V and Taliotis A 2008 *Phys. Rev. D* **78** 115007
- [11] Margotta M, McCarty K, McGahan C, Strickland M and Yager-Elorriaga D 2011 *Phys. Rev. D* **83** 105019
- [12] Barnard N N and Horowitz W A 2017 arXiv:1706.09217
- [13] Kruczenski M, Mateos D, Myers R C and Winters D J 2003 *J. High Energy Phys.* JHEP07(2003)049
- [14] Khachatryan V et al (CMS) 2017 *Phys. Lett. B* **770** 357–9